

PAPER • OPEN ACCESS

Ni-supported palm oil fuel ash catalyst (Ni-POFA) from in situ glycine-nitrate combustion for methane cracking

To cite this article: N H E Hanifa *et al* 2020 *IOP Conf. Ser.: Mater. Sci. Eng.* **736** 042010

View the [article online](#) for updates and enhancements.

Ni-supported palm oil fuel ash catalyst (Ni-POFA) from in situ glycine-nitrate combustion for methane cracking

N H E Hanifa, A Ideris and M Ismail

Faculty of Chemical and Process Engineering Technology, Lebuhraya Tun Razak
Universiti Malaysia Pahang, 26300 Gambang, Pahang, Malaysia

Corresponding author: asmida@ump.edu.my

Abstract. Metal-supported catalysts synthesized using a conventional impregnation method are usually suffered from non-uniform distribution and agglomeration of catalyst particles. In this work, in situ glycine-nitrate combustion method has been explored to synthesize Ni catalyst supported on palm oil fuel ash (Ni-POFA). The properties and performance of the catalyst were compared with one produced using impregnation method. Effects of pre-treatment and catalyst preparation method have been investigated and characterizations of POFA and Ni-POFA catalysts were performed using XRF, XRD, BET surface area, FESEM and TGA. Catalytic activity of the catalysts was evaluated for methane cracking at 550 °C. Results showed that pre-treatment has improved the composition of SiO₂ in POFA from 42.4 to 72.0%. Ni-POFA catalyst synthesized using in situ glycine-nitrate combustion method exhibited a good catalytic performance during the methane cracking with an initial H₂ yield of 6.4%. This was attributed to high Ni metal dispersion on POFA support. Nevertheless, the degradation of CH₄ conversion for this particular catalyst was more significant than one produced using impregnation method. Catalyst prepared using in situ glycine-nitrate combustion was active towards carbon formation, thus led to an obvious formation of carbon on the catalyst surface. Additionally, catalyst preparation method influenced the type of carbon formed on the spent Ni-POFA catalysts.

1. Introduction

Methane steam reforming is a well-known technology and has been extensively applied for H₂ production despite its highly endothermic operation [1, 2]. Additionally, further treatment is required to separate H₂ from other gases containing CO_x, thus contributes to high capital cost and high energy efficiency [3]. As methane steam reforming leads to massive emissions of greenhouse gases (GHGs), technology that utilizes natural gas resources for H₂ production with low GHGs emissions is vital. Methane cracking is another H₂ production technology that is sustainable for H₂ economy since it produces H₂ with zero CO_x emission. The increasing interest amongst researchers towards methane cracking is due to its high methane conversion, the easiness of carbon to be sequestered into a stable solid formed, and its environmental feasibilities [3, 4]. The presence of catalyst in methane cracking significantly reduces the temperature of the reaction process at moderate temperatures compared to the non-catalytic thermal cracking of methane which requires high temperatures up to 1200 °C to obtain a reasonable yield [3].

Ni catalyst has been commonly applied by researchers for methane cracking due to its price and availability [4, 5]. Moreover, Ni has been proven as a very active and stable catalyst for methane



cracking process within the temperature range of 500 – 700 °C [6]. Due to rapid catalyst deactivation caused by large carbon deposition during methane cracking process, the excellent catalyst properties which are highly correlated to catalyst preparation method are crucial for maintaining good catalyst performances and stability [7, 8]. Type of catalyst supports and catalysts preparation method have been reported to a significant effect on Ni supported catalysts. High Ni dispersion, strong metal-support interaction and high surface area have been reported to result in the increase of catalytic performance and stability in methane cracking [7-11]. In previous works, catalysts produced using the conventional method; impregnation have shown several drawbacks. A uniform distribution could not be achieved by this particular method due to the migration of impregnated solution, thus led to the formation of large agglomeration of Ni particles [10]. Additionally, the catalysts produced tend to form less Ni dispersion onto the support [9-11]. These undesirable catalyst properties have led to the search for a better approach of catalyst preparation for Ni supported catalysts.

In situ glycine-nitrate combustion has become an attractive synthesis method for Ni-supported catalyst as it is a rapid and simple process and produces catalysts with high dispersion, high surface area and excellent catalytic activity [12-14]. Kumar et al. [15] have reported that the Cu–Zn catalysts prepared using in situ glycine-nitrate combustion had a larger surface area of double than one produced using co-precipitation method. Cross et al. [14] have applied in situ glycine-nitrate combustion for Ni–SiO₂ catalyst and the catalyst has shown an excellent catalytic activity and stability in ethanol decomposition process. In situ glycine-nitrate combustion method is believed to improve catalytic activity toward reaction process due several advantages such as strong Ni-support interaction and generates catalyst powders with high crystallinity and high surface area [12-14, 16].

Recently, there has been a great interest in utilizing agricultural wastes such as palm oil fuel ash (POFA) [17], eggshell waste [18], and coal fly ash (CFA) [19] in catalytic reactions to make use of their potentials while minimizing the manufacturing costs. Since Malaysia is one of the world's largest producers and exporters of palm oil, POFA is abundantly produced from the combustion of palm oil biomass in the palm oil industries. Normally, POFA is disposed to landfill and the accumulation of this waste has led to environmental pollution problems in the palm oil industries. Since POFA is known for its high amount of SiO₂ [20], the ash exhibits a potential to be developed as a catalyst support for methane cracking. Pre-treatment process of POFA is crucial to improve the POFA morphology while removing the impurities. In previous works on pre-treatment of rice husk and POFA via acid treatment, SiO₂ composition and surface area of the agricultural wastes have been successfully improved [21-23]. Pre-treatment of POFA conducted using HCl solution has resulted in a higher SiO₂ content with 95% in POFA composition [20] compared to one treated via heat treatment method (65%) [24]. Nevertheless, pre-treatment using strong acid is significantly hazardous for environmental and humans which requires a proper disposal treatment.

POFA has a potential to be explored as a catalyst support for methane cracking. Yet, it may contain impurities and the surface structure needs to be tuned into acceptable support properties. In this study, a weak acid; citric acid solution was applied for POFA pre-treatment process and POFA with high SiO₂ content was aimed. The treated POFA was then further utilized as a catalyst support for methane cracking. To address the problems of large agglomerates of particles size and low metal dispersion, the effect of catalyst preparation method also has been investigated. Ni–POFA catalyst was synthesized using in situ glycine-nitrate combustion method and the properties and catalytic performance of the catalyst was compared with one produced using impregnation method.

2. Materials and Methods

2.1. Materials

All chemicals used in this work; citric acid powders (C₆H₈O₇) (M_w=210.14 g/mol) and glycine (NH₂CH₂COOH) (M_w=79.07 g/mol) were purchased from Merck (USA) with purity ≥99 %. Nickel (II) nitrate hexahydrate (Ni(NO₃)₂·6H₂O) (M_w= 290.79 g/mol) for Ni precursor was purchased from Sigma Aldrich (USA).

2.2. Pre-treatment of POFA

The POFA was obtained from Felda Lepar Hilir, Gambang, Pahang, Malaysia. The POFA was initially prepared through drying overnight at 90 °C followed by sieving to obtain the uniform particle size of approximately 71 μm . Pre-treatment of POFA was done by adding the POFA into 1 M of citric acid solution under ultrasonic condition at 42 kHz frequency for 60 min. The slurry was filtered and rinsed with excess distilled water to ensure a neutral pH was obtained. The solid residue of treated POFA was dried at 100 °C for 24 hr to remove moisture and POFA was calcined at 800 °C for 30 min in a furnace.

2.3. Preparation of Ni-POFA catalysts

The Ni-POFA catalysts were using prepared by two preparation methods; a conventional impregnation method and in situ glycine-nitrate combustion. The Ni and POFA weight ratio was at 1: 9 for all prepared Ni-POFA catalyst samples.

2.3.1. Preparation of Ni-POFA catalyst using impregnation method. Treated POFA was impregnated with an aqueous solution of Ni precursor, $\text{Ni}(\text{NO}_3)_2 \cdot 6\text{H}_2\text{O}$ under a continuous stirring at 80 °C for 3 hr. The obtained slurry of impregnated Ni-POFA catalyst was then dried at 100 °C for 12 hr in the oven and calcined at 600 °C for 3 hr. Ni-POFA catalyst synthesized using impregnation method was denoted as Imp Ni-POFA.

2.3.2. Preparation of Ni-POFA catalyst using in situ glycine-nitrate combustion. The nickel nitrate, $\text{Ni}(\text{NO}_3)_2 \cdot 6\text{H}_2\text{O}$ and glycine, $\text{C}_2\text{H}_5\text{NO}_2$ were used as a precursor and fuel, respectively. The solution of nickel nitrate was prepared by dissolving a desired amount of $\text{Ni}(\text{NO}_3)_2 \cdot 6\text{H}_2\text{O}$ in a distilled water. Glycine was added into the nickel nitrates solution with a glycine-nitrates (G/N) ratio of 1.0 to ensure a complete combustion reaction. The POFA was then added into the precursor-glycine media at a fixed Ni: POFA ratio. The mixture solution was then heated at 90 °C on a hot plate under continuous stirring until a gel solution formed. The gel solution was transferred into a ceramic bowl and further heated at approximately 180 °C until the gel was self-ignited and combusted, producing a catalyst ash powder. The catalyst ash powder was then calcined at 600 °C for 3 hr. Ni-POFA catalyst produced from this method was indicated as In situ Ni-POFA.

2.4. Characterization of POFA and Ni-POFA catalysts

The composition of POFA were evaluated using X-ray fluorescence (XRF) spectroscopy of Bruker, S8 Tiger model. The specific surface areas, total pore volume and average pore diameter of the POFA and catalysts were examined using Micromeritics Accelerated Surface Area and Porosimetry analyzer (Model ASAP 2020). The specific areas were obtained using Brunauer-Emmett-Teller, (BET) method whereas total pore volumes and average pore diameter were determined by Barrett-Joyner-Halenda, (BJH) method. The analysis on crystalline structure of the POFA and catalysts were performed using Rigaku Miniflex X-ray Diffractometer (XRD) at 30 kV and 40 mA within the 2θ scanning range of 3° to 80°. The morphology of the fresh and spent catalysts were observed using field emission scanning electron spectroscopy (FESEM) and its elemental surface mapping were analysed via energy dispersive x-ray (EDX) spectroscopy (Model JSM-7800F Schottky Field Emission SEM). The samples were initially placed onto a specimen stub and coated with gold, Au under high vacuum conditions at 15 kV. The accumulation of carbon deposited on the spent catalysts was evaluated using thermo-gravimetric analysis (TGA) in under 60 mL of 6% O_2/N_2 . TGA analysis was performed at temperature from room temperature up to 900 °C at 10 °C/min of heating rate.

2.5. Methane cracking

Methane cracking process of Ni-POFA catalyst was conducted in a fixed-bed reactor inside a quartz tube of 12.7 mm OD and length 433 mm length. A fixed mass of 80 mg catalyst (~125 μm particle

size) was placed on quartz wool in the reactor. The catalyst was reduced under 10 %H₂/N₂ flow at 700 °C for 2 hr prior to the methane cracking reaction. Methane cracking was initiated by switching the reduction gas into the reaction gas (12 mL/min CH₄ and 48 mL/min N₂) and performed at 550 °C for 6 hr. The product gas compositions were analysed using an offline gas chromatography (Agilent 7890B, USA) equipped with thermal conductivity detector (TCD). Catalytic performance of the Ni–POFA catalysts was evaluated using methane conversion (X_{CH_4}) and hydrogen yield (Y_{H_2}) from the following Equations (1) and (2).

$$X_{CH_4} = \frac{n_{CH_4,in} - n_{CH_4,out}}{n_{CH_4,in}} \times 100\% \quad (1)$$

$$Y_{H_2} = \frac{n_{H_2}}{2n_{CH_4,in}} \times 100\% \quad (2)$$

3. Results and Discussions

3.1. Characterization of POFA and Ni–POFA catalyst

Chemical composition of untreated and treated POFA are tabulated in Table 1. The major constituents of untreated POFA consisted of 42.4% silica dioxide (SiO₂), 20.8% calcium oxide (CaO), 12.3% potassium oxide (K₂O) and other metal oxide impurities. The pre-treatment with citric acid solution has improved the SiO₂ content of pre-treated POFA from 42.4 to 72.0% and with the reduction of other oxides. The SiO₂ content in treated POFA this work was slightly lower as compared to previous work from Faizul et al. [20]. 80 – 90 % of SiO₂ was previously achieved when hot plate stirring method was applied during the pre-treatment compared to ultrasonic method in the current work. However, ultrasonication has been reported to have a benefit of higher dispersion of particles thus preventing agglomeration of solid particles [25]. The content of CaO and MgO were significantly reduced by more than half after the pre-treatment with citric acid. This could be related to due to the interaction between the carboxylate ions (RCOO⁻) contain in citric acid with calcium ion (Ca²⁺) and magnesium ion (Mg²⁺) ions [26]. These negative charged of carboxylate ions (RCOO⁻) have been reported to form stable complexes with several metal ions contained in POFA constituents [20], thus resulting in the removal oxides other than SiO₂ in POFA content. Additionally, the color of POFA has changed from dark to greyish colour after the pre-treatment which is expected due to the removal of carbon from POFA constituent. The treated POFA was considered to be rich in SiO₂ and was further utilized for Ni supported catalyst.

Table 1. Chemical composition (%) of untreated and treated POFA.

Items	SiO ₂	CaO	K ₂ O	Fe ₂ O ₃	P ₂ O ₅	MgO	Al ₂ O ₃	Others
POFA (Untreated)	42.4	20.8	12.3	8.0	6.4	3.6	3.0	3.6
POFA (Treated)	72.0	4.8	7.1	7.9	3.5	1.5	2.0	1.3

XRD patterns of untreated POFA and Imp Ni–POFA catalysts produced untreated treated POFA are shown in Fig. 1. All diffraction patterns show the majority of the peaks are corresponded to quartz SiO₂. Similar finding was found by previous works where POFA was composed of crystalline SiO₂ rather than the amorphous SiO [20, 22]. The peak of kalsilite (KAlSiO₄) at 2θ=29° was observed in untreated POFA and Ni–POFA catalyst prepared using untreated POFA (Fig. 1a and 1b). The peak was disappeared in the catalyst prepared using treated POFA (Fig. 1c), suggesting that POFA pre-treatment has successfully removed the impurities available in the POFA, leaving the Ni–POFA catalyst with NiO and SiO₂ quartz peaks only. Moreover, the diffraction peaks of quartz SiO₂ in the catalyst using treated POFA were more obvious than the one prepared using untreated POFA indicated to the POFA pre-treatment has improved the crystallinity of the quartz SiO₂ in Ni–POFA catalyst. In

conclusion, pre-treatment exhibit an improvement on content and crystallinity of quartz SiO_2 in POFA support thus the treated POFA is favourable as a catalyst support for Ni-POFA catalysts.

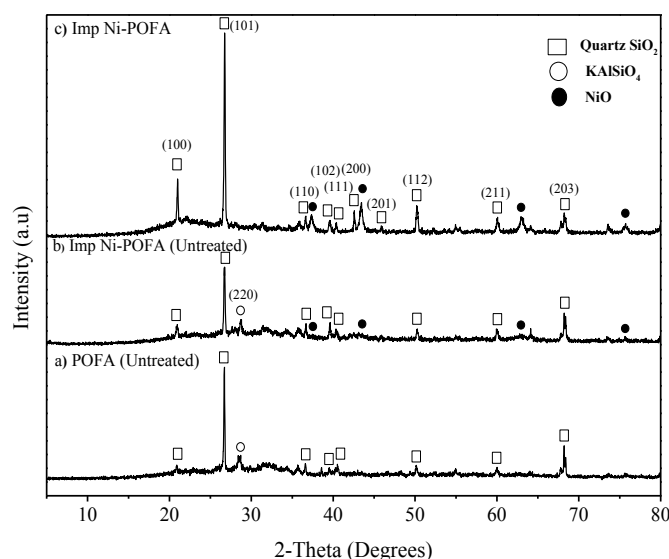


Figure 1. XRD patterns of a) Untreated POFA and Imp Ni-POFA catalysts produced using b) Untreated and c) Treated POFA.

Fig. 2 presents the XRD patterns of Ni-POFA catalysts produced using impregnation (Fig. 2a and 2b) and in situ glycine-nitrate combustion (Fig. 2c and 2d). The unreduced catalysts from impregnation and in situ glycine-nitrate combustion showed the presence of 37° , 43° , 63° and 76° peaks which were corresponding to NiO (111), (200), (220) and (311) planes, respectively (Fig. 2a and 2c). The absence of these peaks in the reduced catalysts revealed that the catalysts were completely reduced and appeared as metallic Ni after reduction process. NiO peaks in the reduced all Ni-POFA catalysts have been replaced by the appearance of new peaks at 45° , 52° , and 76° which are related to Ni (111), (200) and (220) planes (Fig. 2b and 2d). It is important to note that the crystalline intensity of Ni phase for In situ Ni-POFA were slightly lower compared to the one produced using impregnation method (Fig. 2b and 2d). This low crystallinity of metal in metal-supported catalyst is related to high dispersion of the metal catalyst on the support surface [27]. Similar XRD pattern has been reported in Bian et al. where Ni-SiO₂ catalyst produced using impregnation method possessed sharp and narrow intensity of Ni peaks, indicating low Ni dispersion on the SiO₂ support [9]. Therefore, it is believed that Ni-POFA synthesized using in situ glycine-nitrate combustion has a better Ni dispersion over the surface of POFA compared to the one synthesized using impregnation method.

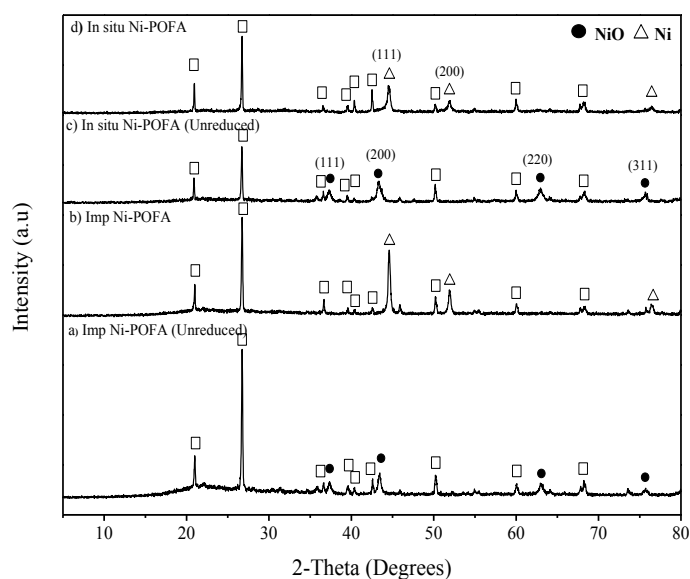


Figure 2. XRD patterns of unreduced and reduced samples of Ni-POFA catalysts produced using a-b) impregnation and c-d) in situ glycine-nitrate combustion.

N₂ adsorption/desorption isotherms plotted in Fig. 3 show that all POFA and in situ Ni-POFA catalysts are corresponded to the type II isotherms. According to the IUPAC classification, both POFA and Ni-POFA catalysts were fitted to the hysteresis loops type H3, which was attributed to a slit-shaped type of pore structures [28]. The same analysis showed that both POFA and Ni-POFA catalysts composed of non-uniform pore size distributions with the range of pores of mesopores (2 – 40 nm) and macropores (50 – 160 nm) size. BET surface areas and pore diameter of POFA and In situ Ni-POFA catalysts are presented in Table 2. The untreated POFA had larger specific surface area compared to the treated POFA. It was observed that enlargement of pore diameter of POFA was observed due to the pre-treatment, that this could be the reason of low specific surface area in treated POFA. Additionally, Ni-POFA catalysts had a higher specific surface area compared to that of POFA alone. This was most probably due to the distributions of Ni particles on the external surface of POFA as a result from the combustion synthesis.

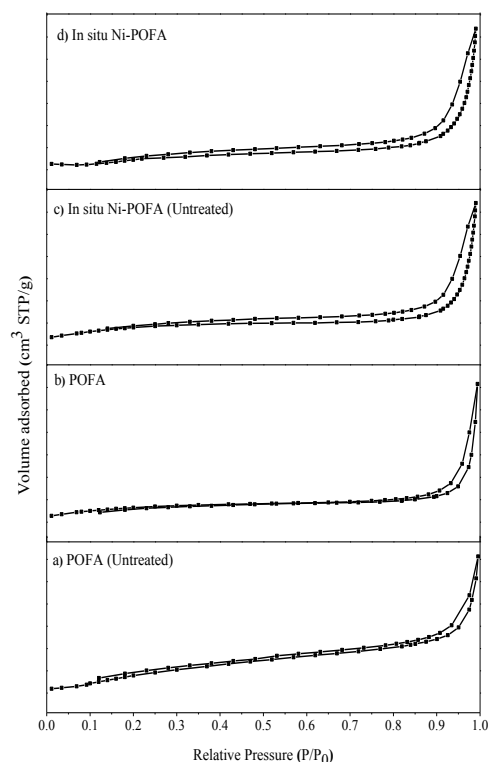


Figure 3. N₂ adsorption/desorption isotherms of a) untreated and b) treated POFA and In situ Ni-POFA catalysts produced using c) untreated and d) treated POFA.

Table 2. Physical properties of POFA and Ni-POFA catalysts.

Catalyst	BET surface area (m ² /g)	Pore diameter (nm)
POFA (Untreated)	5.00	3.95
POFA	2.02	15.09
In situ Ni-POFA (Untreated)	7.90	13.32
In situ Ni-POFA	7.52	16.55

3.2. Catalytic performance of Ni-POFA in methane cracking

Catalytic performance of Ni-POFA catalysts produced using two catalyst preparation methods has been evaluated in methane cracking. H₂ yield and CH₄ conversion of Ni-POFA catalysts were presented in Fig. 4. Ni-POFA catalysts synthesized using in situ glycine nitrate combustion (In situ Ni-POFA) exhibited a higher H₂ yield with an initial of 6.4% compared to the Ni-POFA catalyst synthesized using impregnation (Imp Ni-POFA) with 2.5%. Both catalysts nevertheless showed a rapid degradation of H₂ yield over time. A better H₂ yield at the beginning of the reaction by In situ Ni-POFA can be ascribed to the high availability of the Ni active sites on the catalyst that were exposed to the CH₄ gas molecules. This attributed to high Ni dispersion on the POFA surface as supported by XRD analysis in Fig. 2. However, an inverse trend was observed for CH₄ conversion when the conversion of In situ Ni-POFA was rapidly decreased over time while the value was stable at 35.0% for Imp Ni-POFA catalyst. It is suggested that In situ Ni-POFA is not only active for H₂ production but also towards the formation of carbon which has blocked the Ni sites, causing a higher degradation in the particular catalyst. In comparison with other works on methane cracking at 550 °C, Ni supported on bimodal porous silica (Ni-BPS) catalyst exhibited the CH₄ conversion and H₂ yield in the range of 2.5 – 20.0 % and 3.0 – 15.0 %, respectively [8]. Takaneke et al. [29] used Ni-SiO₂ catalyst in methane cracking and the highest CH₄ was achieved at only 8.0% yet its stability was longer for 80 hr reaction

time. As catalytic performance of Ni-POFA catalysts was found to be better than previous works using commercialized SiO_2 , Ni-POFA catalyst has a potential to be explored for H_2 production catalyst through methane cracking reaction.

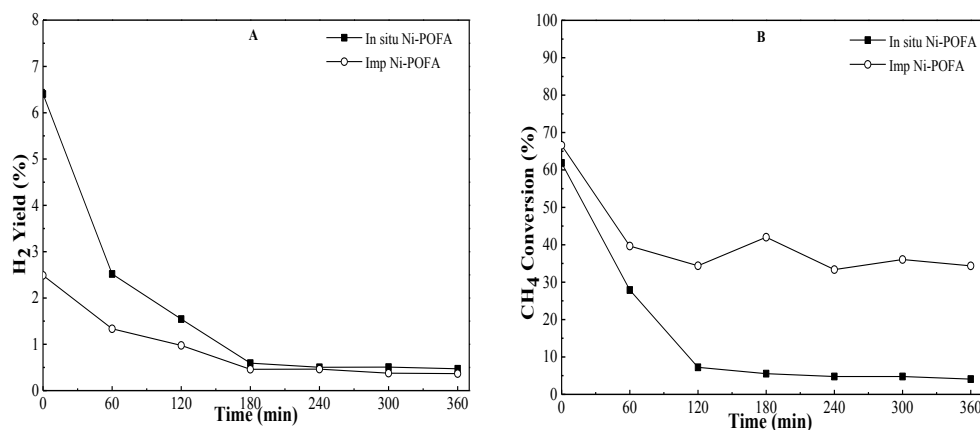


Figure 4. a) H_2 yield and b) CH_4 conversion for Ni-POFA catalysts synthesized using impregnation (Imp Ni-POFA) and in situ glycine nitrate combustion (In situ Ni-POFA) during methane cracking at 550°C .

The morphology of fresh and spent Ni-POFA catalysts produced using impregnation and in situ glycine nitrate combustion method is shown in Fig. 5. Obviously, the morphology of both Imp Ni-POFA and In situ Ni-POFA catalysts was highly influenced by the catalyst preparation method. In the fresh catalysts, material with greyish in color was belong to POFA support while material with brighter in colour was belong to Ni particles (Fig. 5a and Fig. 5c). Ni particles in the Imp Ni-POFA catalyst were round-shape in structure while the Ni particles for In situ Ni-POFA catalyst were in randomly-shape with the Ni particles are linked between each other. Ni particles were distributed all over the POFA surface for both Ni-POFA catalysts and the Ni particles only deposited on the external surface of POFA, giving a larger specific surface area of catalyst than its POFA support alone. The distribution of Ni particles on Imp Ni-POFA were very close to each other which can led to particle agglomeration. Similar morphology was obtained in Lazaro et al. [10] for the Ni- SiO_2 catalyst prepared using impregnation method, where the Ni particles tend to agglomerate, forming larger particles. Effect of agglomeration on Imp Ni-POFA was obvious in its spent catalyst (Fig. 5b). In situ Ni-POFA catalyst on the other seems to have high metal dispersion thus high availability of Ni active sites on POFA support. This is related to the high catalytic activity thus higher H_2 yield in In situ Ni-POFA catalyst.

High catalytic activity may also lead to high carbon formation on catalyst surface. This is true for In situ Ni-POFA catalyst where it produced more carbon on its surface. An obvious accumulation of filamentous-types of carbon was observed on the surface of In situ Ni-POFA catalyst, which could be the main reason the higher degradation rate of CH_4 conversion of In situ Ni-POFA catalyst (Fig. 5b). On the other hand, formation of large agglomerate of Ni particles found on the spent Imp Ni-POFA may have caused the low activity of the catalyst with carbon formed the surface is encapsulated carbon. This suggests that catalyst preparation method influences the type of carbon formed on spent Ni-POFA catalysts.

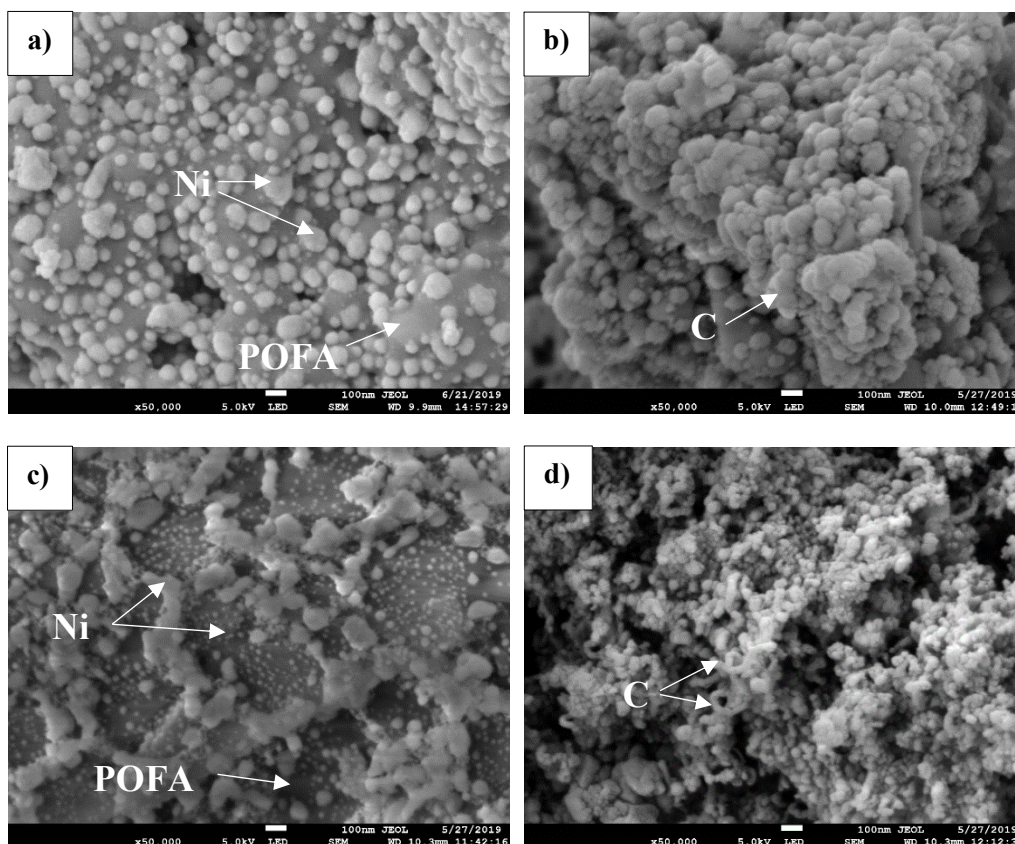


Figure 5. FESEM micrographs of fresh and spent Ni-POFA catalysts produced using a-b) impregnation and c-d) in situ glycine-nitrate combustion method

The TGA curves in Fig. 6 show the percentage of weight loss in spent Ni-POFA catalysts. The weight loss was observed on the spent In situ Ni-POFA catalyst at temperature range of 450 – 550 °C (Fig. 6b). This is corresponding to the oxidation of deposited carbon from the catalyst surface. Meanwhile, there was no weight loss observed for Imp Ni-POFA catalyst suggesting that the amount of carbon deposited on Imp Ni-POFA was almost negligible compared to one deposited on In situ Ni-POFA catalyst (Fig. 6a). On the other hand, an increasing weight in Imp Ni-POFA catalyst was found at temperature above 500 °C, probably due to the oxidation of Ni species to NiO species on the catalyst at high temperatures. This analysis suggests that In situ Ni-POFA was not only active for H₂ production but also in carbon formation, resulted in more carbon deposition on its surface.

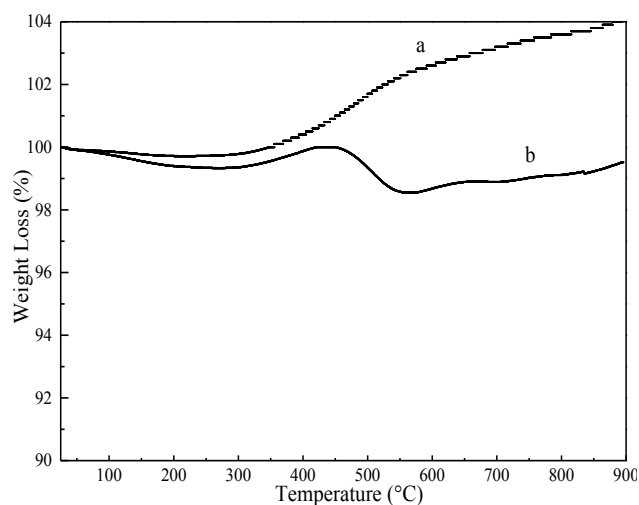


Figure 6. TGA curves of spent Ni-POFA catalysts produced using a) impregnation and b) in situ glycine-nitrate combustion method

4. Conclusions

Pre-treatment of POFA with citric acid solution has improved the SiO₂ content in the POFA support from 42.4 to 72.0% and increased the crystallinity of the quartz SiO₂ in POFA. Effect of catalyst preparation method was evaluated for pre-treated POFA catalysts using in situ glycine-nitrate combustion and impregnation method. Ni-POFA prepared using in situ glycine-nitrate combustion had a better initial H₂ yield (6.4%) than the one synthesized using conventional impregnation method (2.5%). This better catalytic activity was ascribed to higher Ni dispersion of Ni-POFA catalyst prepared using in situ glycine-nitrate combustion. However, higher degradation rate of CH₄ conversion and higher amount of carbon was found with methane cracking using In situ Ni-POFA catalyst. This suggests that Ni-POFA catalysts synthesized by in situ glycine-nitrate combustion was active for both H₂ production and carbon formation. Filamentous carbon was found on the spent In situ Ni-POFA while encapsulating carbon was observed on the Imp Ni-POFA suggesting that catalyst preparation method influenced the type of carbon formed. In summary, in situ glycine-nitrate combustion employed for the synthesis of Ni-POFA catalyst has improved the dispersion Ni metal particles of the catalyst and exhibited an active catalytic activity in methane cracking.

Acknowledgement

Authors would like to acknowledge the funding received from Ministry of Education Malaysia for work under Fundamental Research Grant Scheme (FRGS/1/2017/TK02/UMP/02/18) (RDU170119).

References

- [1] Chen Y, Zhou W, Shao Z and Xu N, 2008 *Catal. Commun.* **9** 1418-25
- [2] Armor J N, 1999 *Appl. Catal., A*. **176** 159-76
- [3] Abbas H F and Daud W M A W, 2010 *Int. J. Hydrogen Energy*. **35** 1160-90
- [4] Rastegarpanah A, Rezaei M, Meshkani F, Dai H and Arandiyani H, 2018 *Int. J. Hydrogen Energy*. **43** 15112-23
- [5] Ewald S, Standl S and Hinrichsen O, 2018 *Appl. Catal., A*. **549** 93-101
- [6] Amin A M, Croiset E and Epling W, 2011 *Int. J. Hydrogen Energy*. **36** 2904-35
- [7] Amin A M, Croiset E, Constantinou C and Epling W, 2012 *Int. J. Hydrogen Energy*. **37** 9038-48
- [8] Donphai W, Phichairatanaphong O, Klysubun W and Chareonpanich M, 2018 *Int. J. Hydrogen*

- Energy*. **43** 21798-809
- [9] Bian L, Zhao T, Zhang L and Li Z, 2018 *Appl. Surf. Sci.* **455** 53-60
- [10] Lazaro M J, Echegoyen Y, Suelves I, Palacios J M and Moliner R, 2007 *Appl. Catal., A*. **329** 22-29
- [11] Echegoyen Y, Suelves I, Lazaro M J, Sanjuan M L and Moliner R, 2007 *Appl. Catal., A*. **333** 229-37
- [12] Dinka P and Mukasyan A S, 2005 *J. Phys. Chem. B*. **109** 21627-33
- [13] Kumar A, Cross A, Manukyan K, Bhosale R R, Van Den Broeke L J P, Miller J T, Mukasyan A S and Wolf E E, 2015 *Chem. Eng. J.* **278** 46-54
- [14] Cross A, Roslyakov S, Manukyan K V, Rouvimov S, Rogachev A S, Kovalev D, Wolf E E and Mukasyan A S, 2014 *Journal of Physical Chemistry C*. **118** 26191-98
- [15] Kumar A, Miller J T, Mukasyan A S and Wolf E E, 2013 *Appl. Catal., A*. **467** 593-603
- [16] Varma A, Mukasyan A S, Rogachev A S and Manukyan K, 2016 *Chem. Rev.* **116** 14493-586
- [17] Chong C C, Abdullah N, Bukhari S N, Ainirazali N, Teh L P and Setiabudi H D, 2018 *Int. J. Hydrogen Energy*.
- [18] Wei Z, Xu C and Li B, 2009 *Bioresour. Technol.* **100** 2883-85
- [19] Asl S M H, Ghadi A, Baei S M, Javadian H, Maghsudi M and Kazemian H, 2018 *Fuel*. **217** 320-42
- [20] Faizul C P, Abdullah C and Fazlul B, 2013 *In Advanced Materials Research*. **626** 997-1000
- [21] Carmona V B, Oliveira R M, Silva W T L, Mattoso L H C and Marconcini J M, 2013 *Industrial Crops and Products*. **43** 291-96
- [22] Kongnoo A, Tontisirin S, Worathanakul P and Phalakornkule C, 2017 *Fuel*. **193** 385-94
- [23] Bakar R A, Yahya R and Gan S N, 2016 *Procedia Chemistry*. **19** 189-95
- [24] Johari M M, Zeyad A M, Bunnori N M and Ariffin K S, 2012 *Construction and Building Materials*. **30** 281-88
- [25] Zhang N, Zhang G, Chong S, Zhao H, Huang T and Zhu J, 2018 *Journal of Environmental Management*. **205** 134-41
- [26] Umeda J and Kondoh K, 2008 *Journal of Materials Science*. **43** 7084-90
- [27] Yan Y, Dai Y, Yang Y and Lapkin A A, 2018 *Appl. Catal., B*. **237** 504-12
- [28] ALOthman Z, 2012 *Materials*. **5** 2874-902
- [29] Takenaka S, Kobayashi S, Ogihara H and Otsuka K, 2003 *J. Catal.* **217** 79-87